KAWASAKI STEEL TECHNICAL REPORT
No.25 (September 1991)
Special Issue on 'H-Shapes with Fixed Outer Dimension' and 'Steel Pipe'

Production and Properties of Seamless Modified 9Cr-1Mo Steel Boiler Tubes

Terufumi Sasaki, Kunihiko Kobayashi, Teruo Yamaura, Toshiaki Kasuya, Toshikazu Masuda

---

Synopsis :
The production of seamless modified 9Cr-1Mo steel tube by the Mannesmann process was studied regarding the hot workability and heat-treatment conditions. The mechanical properties of the base metal and welded joints, and the Charpy absorbed energy and precipitation behavior after long-time aging were also investigated. The hot workability of modified 9Cr-1Mo(T91) steel was found to be inferior to that of low-alloy steel, but the steel tube and pipe can be produced by optimizing the rolling conditions and by reducing the S content. The tensile strength at elevated temperatures and the creep rupture strength of T91 steel pipe were excellent and satisfied ASME specifications. The tensile, impact, and bending properties of mechanized GTAW girth welded joints were sufficiently good. The Charpy absorbed energy of T91 steel pipe decreased after aging at 550-650℃, but retained a good enough value, this decrease being most marked at 600℃ due to the increase in coarse (FeCr)2Mo precipitates identified by SEM observation. Hot-finished tube produced by the Mannesmann process showed equivalent properties to those of cold-finished tube, with sufficient dimensional accuracy.

The body can be viewed from the next page.

Production and Properties of Seamless Modified 9Cr-1Mo Steel Boiler Tubes*

Terufumi Sasaki
Dr. Sci., Senior Researcher, Tubular Products Lab., Heavy Steel Products Res. Dept., Iron & Steel Res. Labs.

Kunihiko Kobayashi
Staff General Manager, Planning & Administration Sec., Research Planning Dept.

Teruo Yamaura
Senior Researcher, Joining & Physical Metallurgy Lab., Heavy Steel Products Res. Dept., Iron & Steel Res. Labs.

Toshiaki Kasuya
Staff Assistant Manager, Pipe Technology Sec., Manufacturing Dept., Chita Works

Toshikazu Masuda
Staff Manager, Technical & Quality Control Sec., Technology & Production Control Dept., Chita Works

Synopsis:

The production of seamless modified 9Cr-1Mo steel tube by the Mannesmann process was studied regarding the hot workability and heat-treatment conditions. The mechanical properties of the base metal and welded joints, and the Charpy absorbed energy and precipitation behavior after long-time aging were also investigated. The hot workability of modified 9Cr-1Mo(T91) steel was found to be inferior to that of low-alloy steel, but the steel tube and pipe can be produced by optimizing the rolling conditions and by reducing the S content. The tensile strength at elevated temperatures and the creep rupture strength of T91 steel pipe were excellent and satistied ASME specifications. The tensile, impact, and bending properties of mechanized GTAW girth welded joints were sufficiently good. The Charpy absorbed energy of T91 steel pipe decreased after aging at 550-650°C, but retained a good enough value, this decrease being most marked at 600°C due to the increase in coarse $(FeCr)_2Mo$ precipitates identified by SEM observation. Hot-finished tube produced by the Mannesmann process showed equivalent properties to those of cold-finished tube, with sufficient dimensional accuracy.

1 Introduction

Seamless modified 9Cr-1Mo steel tubes and pipes (ASME SA 213 T91 and SA 335 P91) are being increasingly used in boilers operated at high temperatures. Many trials on the production and fabrication for application to boilers have been reported for this steel.[1-7] High-alloy steel tubes are generally manufactured by the hot extrusion process due to the poor hot workability, and modified 9Cr-1Mo steel tubes are usually produced by this process. However, the Mannesmann process is superior to the extrusion process in production efficiency and dimensional accuracy. One problem with the latter process is scoring which appears easily at the rolling stages of the piercing mill and mandrel mill. The newly developed MAP system[8] (mandrel mill pass schedule design system) has solved the problem for the mandrel mill by adopting a suitable caliber design and appropriate rolling schedule. The piercing mill, on the other hand, still requires a suitable solution for the problem.

Cold-finished tubes have traditionally been used for superheaters and reheaters owing to their good dimensional accuracy and low internal surface roughness, but the adoption of hot-finished tube has recently been increasing. This is due to the development of better hot-finished tube with good dimensional accuracy as well as to the economic advantages. Kawasaki Steel has developed the method for producing modified 9Cr-1Mo tube by the Mannesmann process and has gained considerable experience in its production and application.

This paper reports a study on the hot workability and

* Originally published in *Kawasaki Steel Giho*, **22**(1990)4, 257-265

heat treatment required in the production of T91 steel tube and P91 pipe, as well as various other properties.

2 Materials and Experimental Method

2.1 Materials

The chemical compositions of the steels produced from 100 kg ingots for the laboratory tests are shown in **Table 1**. No.1 steels were used for the Gleeble test with varying S contents from 0.001 to 0.003 mass %, and No.2 and No.3 steels, which correspond to ASME SA 213 T9 and T1 steels respectively, were tested for comparison. The effects on mechanical properties of heat treatment conditions for normalizing and tempering temperature were studied with No.4 steel.

The sizes and chemical compositions of the tested mill products are shown in **Table 2** as A~D. Steels A, C and D were seamless cold-finished tubes produced by the Mannesmann mandrel mill process with subsequent cold drawing, and steel B was a seamless hot-finished pipe produced by the Mannesmann plug mill process.

An example of the size and chemical composition of hot-finished tube for testing is shown as E in Table 2.

2.2 Experimental Methods

2.2.1 Hot workability

Hot workability was evaluated for the critical reduction by the Mannesmann effect with a model piercing mill test or for the reduction of diameter by a high-temperature/high-speed tensile test (the Gleeble test).

2.2.2 Properties of the cold-finished tube and hot-finished pipe

Various tests were performed: cross sectional microstructure test; flattening and flaring tests; high temperature tension and creep rupture tests with round bar of 6-mm diameter and 30-mm GL test pieces taken from mid thickness for longitudinal direction; ash corrosion test with synthetic ashes; welded joint test; and impact test after long time aging.

Both similar welded joints in T91 and dissimilar joints in T91 and STBA24 were tested. **Table 3** shows the tubes that were tested for mechanized GTAW girth welding, and **Table 4** shows the chemical composition of the materials tested.

2.2.3 Properties of the hot-finished tube

Measurements of the dimensional accuracy, flattening and flaring characteristics, and mechanical properties were taken.

Table 3 Base metal and welding material for similar and dissimilar joints

	Tested tube	Welding material
Similar joint	SA213 T91/SA213 T91	KT-9 CM(1.2 mm ϕ)
Dissimilar joint	SA213 T91/STBA 24	KT-2 CM(1.2 mm ϕ)

Table 1 Chemical compositions of steels for laboratory tests (mass %)

Steel No.	C	Si	Mn	P	S	Cr	Mo	Nb	V	N	ASME
1	0.09	0.35	0.40	0.015	0.001~0.003	9.0	1.0	0.09	0.20	0.04	T91
2	0.11	0.49	0.43	0.010	0.004	8.9	1.0	—	—	0.01	T9
3	0.15	0.23	0.51	0.014	0.008	—	0.54	—	—	—	T1
4	0.09	0.30	0.43	0.008	0.003	9.1	1.0	0.08	0.20	0.04	T91

Table 2 Sizes and chemical compositions of the tested mill products

Steel	Size (mm)	Chemical composition (mass %)										Products
		C	Si	Mn	P	S	Cr	Mo	Nb	V	N	
A	50.8 ϕ × 10.8 t	0.10	0.39	0.39	0.008	0.003	8.46	1.01	0.078	0.20	0.038	Cold-finished tube
B	355.6 ϕ × 22 t	0.10	0.39	0.39	0.008	0.003	8.46	1.01	0.078	0.20	0.038	Hot-finished pipe
C	50.8 ϕ × 5.0 t	0.09	0.27	0.44	0.008	0.002	9.15	0.99	0.080	0.20	0.041	Cold-finished tube
D	50.8 ϕ × 6.0 t	0.09	0.36	0.37	0.008	0.004	8.50	0.99	0.079	0.20	0.034	Cold-finished tube
E	42.4 ϕ × 4.5 t	0.10	0.37	0.32	0.018	0.002	8.60	0.93	0.077	0.19	0.037	Hot-finished tube

Table 4 Chemical compositions of base metal and welding material for similar and dissimilar joints (mass %)

Tested material	C	Si	Mn	P	S	Cr	Mo	Ni	Nb	V	N (ppm)
SA 213 T 91*1	0.10	0.39	0.39	0.008	0.003	8.46	1.01	0.10	0.078	0.195	430
STBA 24*1	0.12	0.34	0.44	0.009	0.005	2.10	0.98	0.03	—	—	68
KT-9 CM	0.08	0.30	0.79	0.002	0.002	9.27	1.01	0.67	0.022	0.150	140
KT-2 CM	0.12	0.30	0.75	0.002	0.003	2.49	1.06	—	—	—	16

*1 50.8 mm ϕ × 10.8 mm t

3 Experimental Results and Discussion

3.1 Laboratory Experiments on Hot Workability

The critical reduction by the Mannesmann effect on T91 steel was about 7–12%, being inferior to that of T9 steel, which is about 17%. It is necessary to possess good workability at 950–1200°C for producing tube and pipe by the Mannesmann process. Gleeble test results on T91 steel with various S contents are shown in **Fig. 1**, in comparison with T9 and T1 steels. The figure shows that T91 steel was inferior to T9 and low-alloy steel in its hot workability, and that reducing the S content was effective for improving hot workability at 1150–1250°C. In addition to reducing the S content for mill production of T91 and P91 steel, the billet heating temperature, roll gap, and the setting position and surface temperature of the plug in the piercing mill were optimized by Kawasaki Steel to establish the best method for producing this steel tube and pipe without internal defects.

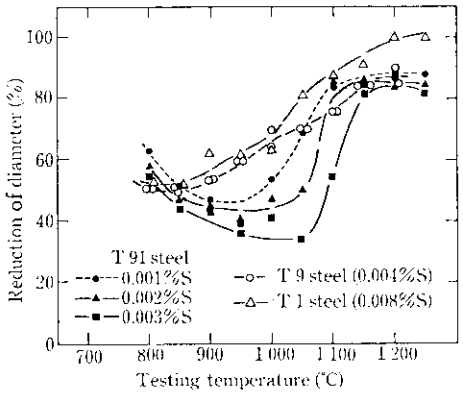

Fig. 1 Temperature dependence in reduction of diameter of T91 by Gleeble test

3.2 Laboratory Tests on Normalizing and Tempering Conditions

The CCT curve for T91 steel was first examined before studying the heat treatment conditions and is shown in **Fig. 2**. The M_s temperature is about 400°C and the Vickers hardness is almost constant over a wide range of cooling times to 10^4 s.

The effects of heat treatment conditions on the mechanical properties were studied by changing the normalizing temperature from 1000 to 1075°C and the tempering temperature from 730 to 820°C. Both the 0.2% PS and TS were a little higher after normalizing at 1050°C or higher than after normalizing at 1025°C or

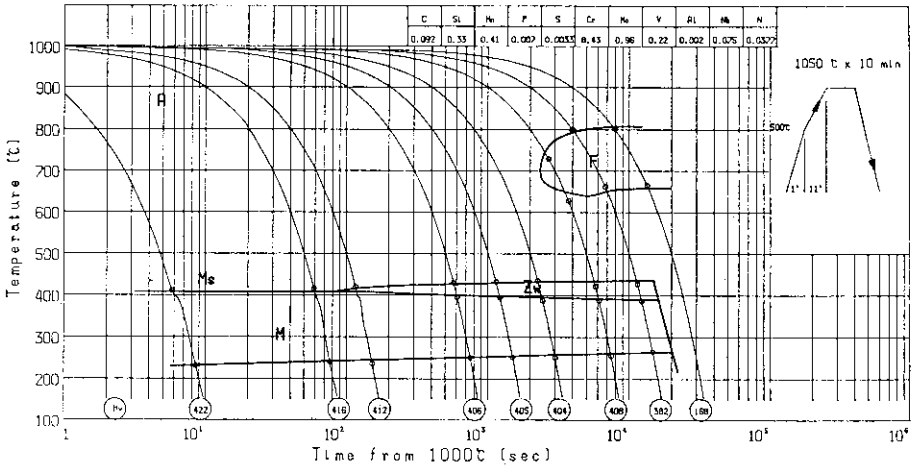

Fig. 2 CCT diagram of T91

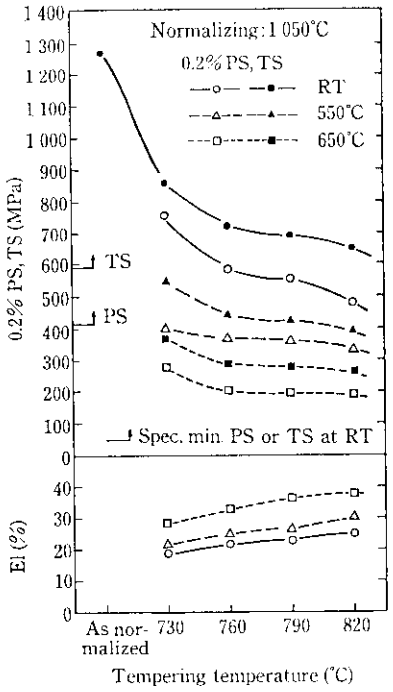

Fig. 3 Influence of tempering temperature on mechanical properties

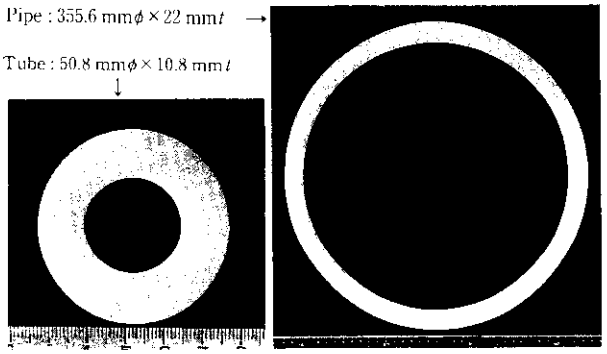

Photo 1 Macrostructure of modified 9Cr-1Mo tube and pipe

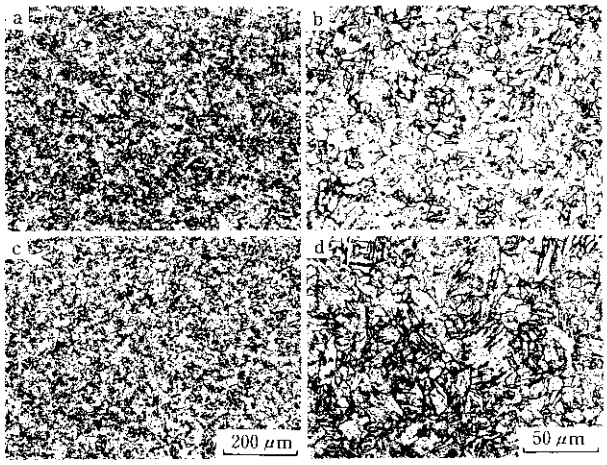

a, b : 50.8 mmφ × 10.8 mmt

c, d : 355.6 mmφ × 22 mmt

Photo 2 Microstructure of modified 9Cr-1Mo tube and pipe

lower, but the normalizing temperature had little effect on the tensile properties. The specification of HRC being less than or equal to 25 was not satisfied when tempered at 730°C or lower for all normalizing temperatures. The mechanical properties of this steel when normalized at 1050°C and tempered at between 730 and 820°C are shown in **Fig. 3**. The tensile strength was higher after tempering at 730°C or less and decreased greatly after tempering at 820°C. Optimum strength could be obtained by tempering between 760 and 790°C, with little dependence on the tempering temperature within this range.

These experiments indicated that the optimum normalizing temperature was 1050°C, which is the critical temperature to avoid coarsening of the austenite grains, and that the optimum tempering temperature lay between 760 and 790°C.

3.3 Properties of Cold-Finished Tube and Hot-Finished Pipe

The normalizing and tempering temperatures were chosen as 1050 and 790°C, respectively, based on the foregoing results.

3.3.1 Macro- and microstructure

Examples of the macro- and microstructure of the tube and pipe are shown in **Photos 1** and **2**. Both the tube and pipe show a uniformly tempered martensitic structure, and the cross-sectional photograph shows no defects and a good shape.

3.3.2 Flattening and flaring tests

Photo 3 shows the test results after flattening and flaring of tube A. No cracking was observed after contact-flattening, and good elongation of more than 280% was obtained in the flaring test.

3.3.3 Mechanical properties at elevated temperatures

The results of tensile tests at elevated temperatures are shown in **Fig. 4** for the L-direction of the tube and C-direction of the pipe. The same strength properties were obtained independent of the product size or test direction equivalent to the figures obtained in other tests. Figure 4 also shows the minimum value of 0.2% PS and TS reported by Oak Ridge National Laboratory (ORNL), the obtained values being sufficiently high compared to the ORNL values.

The results of creep rupture tests are shown in **Fig. 5**, the average value line and minimum value line also

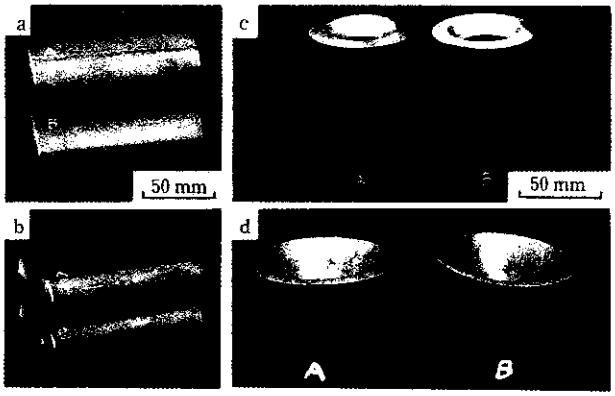

Flattening test
a : First step, no crack
$H \leq 40.9$ mm
b : Second step (contact), no crack
$H = 26.5$ mm

Flaring test
c : First step, no crack
Expansion rate = 1.38
d : Second step (crack initiation)
Expansion rate = 2.95

Photo 3 Appearance of flattening and flaring tested specimens

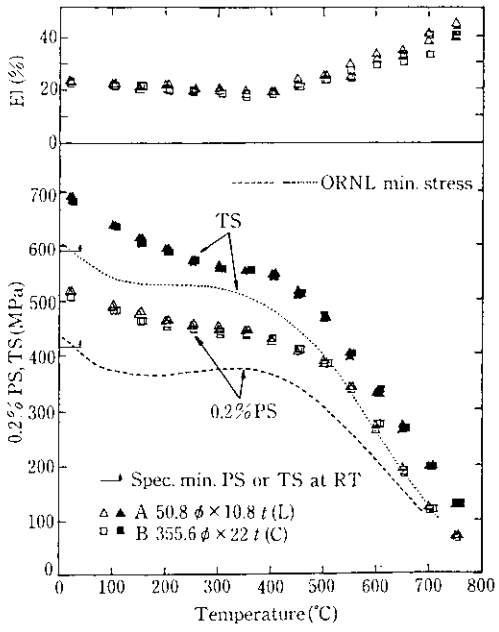

Fig. 4 Temperature dependence of short time tensile properties

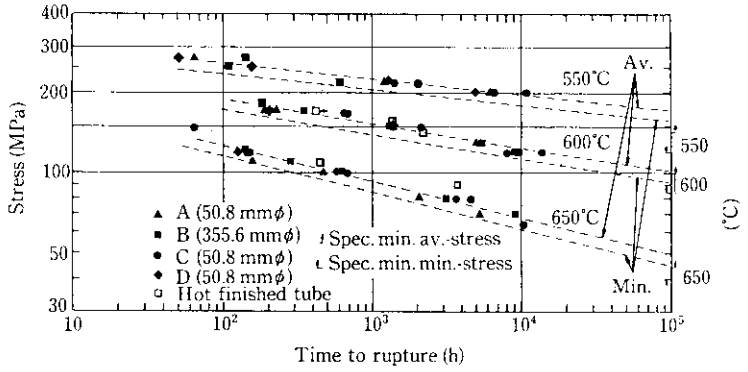

Fig. 5 Stress–time to rupture curves at 550, 600, and 650°C

being shown. Linear extrapolated values to 10^5 h satisfy the minimum values calculated from the ASME maximum allowable stress, which is shown on the right-hand side of the figure.

3.3.4 Properties of welded joints

Welding was done by mechanized GTAW girth welding, the first layer being welded without preheating (welding current 140–220A, welding voltage 11–13V) after which 8 layers were welded in 2 passes with an inter-pass temperature below 250°C.

Table 5 shows the tensile and bending test results on the welded joints after a post-weld heat treatment (PWHT) of 740°C for 1h. The fracture position in the similar-metal joints was in the base metal and the tensile strength of the joint was the same as that of the base metal. The fracture position in the dissimilar metal joints was in the STBA24 base metal. No cracking was observed after the bending test.

Table 5 Test results of welded joints

Condition of PWHT	Welded joint	Tensile test (JIS Z 3121)		Bend test (JIS Z 3122)	
		TS (MPa)	Fracture position	Face	Root
740°C×1 h (TP=20.3)	Similar (T 91/T 91)	70.7	BM	Good	Good
		69.4	BM	Good	Good
	Dissimilar (T 91/ STBA 24)	53.9	BM (STBA 24)	Good	Good
		53.2	BM (STBA 24)	Good	Good

Figure 6 shows the Charpy impact test results from

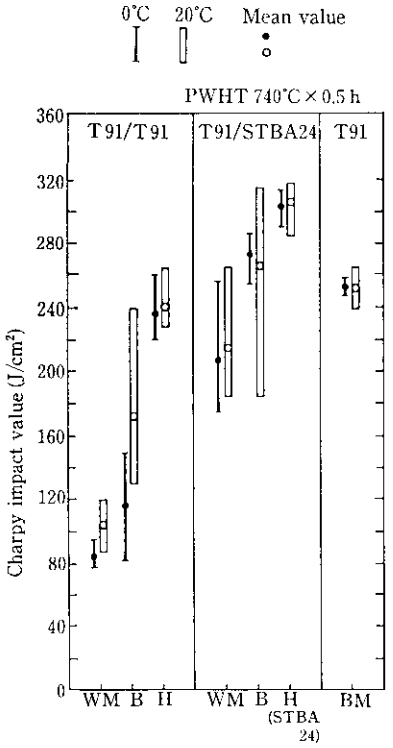

Fig. 6 Charpy impact value of welded joints

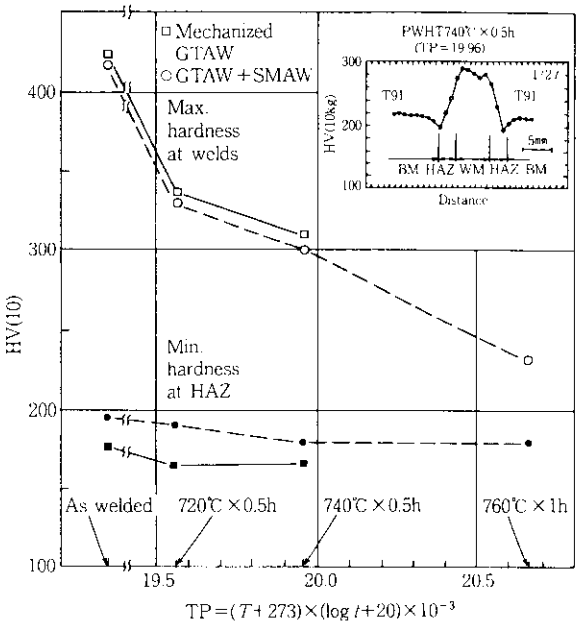

Fig. 7 Change in hardness at welds and HAZ with PWHT temperature T(°C) and time t(h)

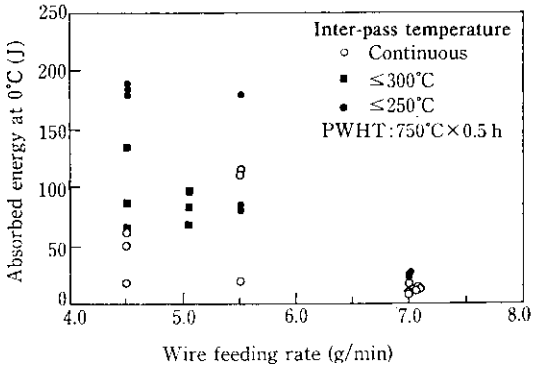

Fig. 8 Influence of wire feed rate and inter-pass temperature on absorbed energy of welds

the similar and dissimilar metal joints after PWHT of 740°C for 0.5h. The impact value was highest in HAZ, next at the bond, and lowest in the weld metal (WM) for both the similar and dissimilar metal welded joints. The impact value for WM of the similar metal joints was more than 80 J/cm^2, and that of the dissimilar metal joints was more than 160 J/cm^2, these values being satisfactory. Good matching was confirmed between dissimilar welding materials of T91 and STBA24 steels when using STBA24 welding material. **Figure 7** shows the maximum and minimum hardness dependence on the PWHT conditions, the maximum hardness decreasing to less than Hv 300 with a tempering parameter (TP) greater than 20.0. Softening in HAZ was observed in the hardness distribution, but the fracture position in the tensile tests were confirmed not to be in this softened area as already mentioned.

The recovery of impact energy in the girth welded joint of a boiler tube might be insufficient due to the comparatively short time for PWHT. In such a case, it is necessary to improve the absorbed energy in the as-welded condition. **Figure 8** shows the influence of wire feed rate and inter-pass temperature on the absorbed energy of the weld metal. In the case of a high wire feed rate such as 7 g/min, the absorbed energy is low for both continuous welding and at a low inter-pass temperature of less than 250°C. The absorbed energy can be greatly increased by controlling the inter-pass temperature with a decreased wire feed rate, this increase being more marked when the inter-pass temperature is less than 250°C. A fine microstructure is obtained due to the reheating effect when the inter-pass temperature less than 250°C.

It is most effective to control inter-pass temperature to less than the M_s temperature, or preferably less than 250°C, and to control the wire feed rate to less than about 5 g/min.

3.3.5 Ash corrosion test

Test results of hot corrosion by synthetic ash are shown in **Fig. 9**, with the figures for STBA24 and SUS321H added for comparison. The experimental conditions for the synthetic ash and gas compositions and for the SO_2 content are shown in the figure. The corro-

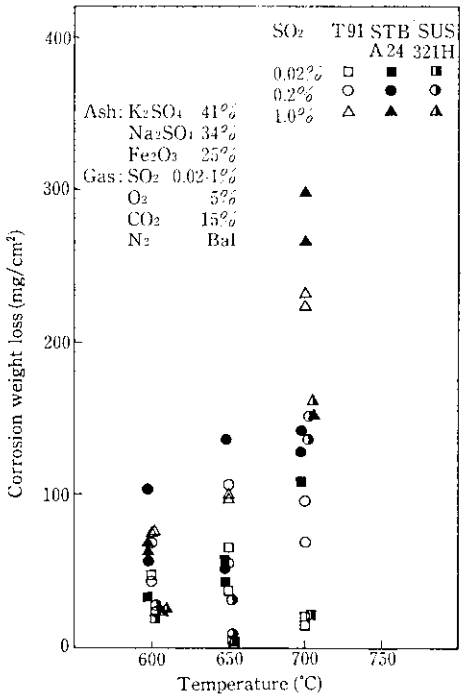

Fig. 9 Corrosion weight loss by ash corrosion test

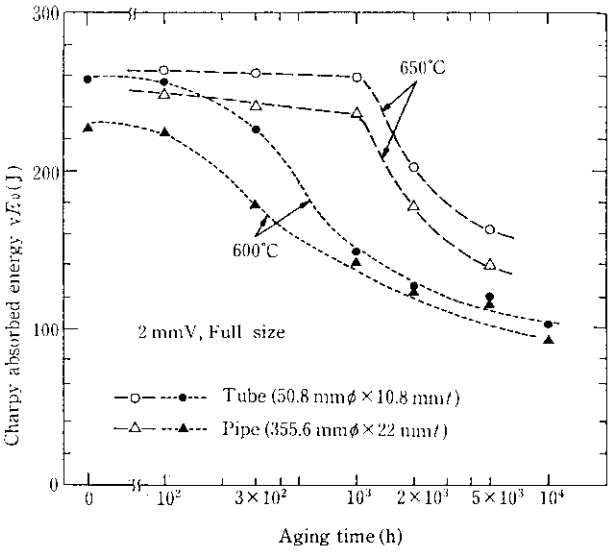

Fig. 10 Change in Charpy absorbed energy with aging time and temperature

sion resistance of T91 steel was between those of STBA24 and SUS321H, and it increased with Cr content.

3.3.6 Precipitates and impact properties after aging

It has been pointed out that the impact energy of 9-12Cr steel decreased with aging time, and that this behavior was closely related to precipitates.[9-14] Many suggestions for the decrease in impact energy with aging treatment were pointed out concerning such aspects as coarsening of $M_{23}C_6$ precipitates, an increase in precipitates of mainly $M_{23}C_6$ carbide, and the precipitation of Fe_2Mo, but no decisive reason was presented. A study on the effect of long-term aging on impact energy change has been performed in detail at 550°C, but few studies have been performed on this steel at 600°C or 650°C that can be used to assess an accelerating precipitation behavior above that at 550°C. As boiler tube is used for a long time at high temperatures, the relationship between the change of microstructure (especially the morphology) and the amount of precipitates and the impact property was studied to better understand the effect of long-term aging.[15]

The change of Charpy absorbed energy at 0°C, $_vE_0$, after aging for 1000h at between 550 and 650°C was examined. There was no clear change until after 100h, but the absorbed energy decreased in a temperature range of 550-625°C after more than 300h, and decreased further excluding aging at 650°C for 1000h. On the bases of this findings, long-term aging was performed at 600 and 650°C, the changes of $_vE_0$ for specimens aged at 600 and 650°C being shown in **Fig. 10**. Here, $_vE_0$ decreased with increased aging time at 600°C after more than 100h, and was particularly marked till 2000h. However, $_vE_0$ was about 100J even after aging for 10000h and this is a satisfactory value in practice. The $_vE_0$ decreased after more than 1000h aging at 650°C, but the decrement was smaller than that at 600°C.

The change in composition of the residue extracted from the specimens after aging at 550-650°C for 100-1000h and longer at 600°C is shown **Fig. 11**. The contents of V and Nb were constant independent of aging time at any temperature. The contents of Cr, Fe and Mo increased with increasing aging time at 550 and 600°C, while that of Fe decreased at 650°C. The extracted residues increased with increasing aging time, the increment being largest at 600°C.

Several reasons for the change of impact properties after long-term aging are possible: (1) change in the tempered martensitic structure, (2) change in the hardness (strength), and (3) change in the amount, morphorogy, size and site of precipitates. No obvious change was observed in the tempered martensitic structure, and almost no change was observed in the Vickers hardness.

The relationship between the increments of Mo and Fe+Cr contents in the residue in the normalized and tempered condition is shown in **Fig. 12**. The data fit well with the calculated line obtained by assuming the formation of Fe_2Mo as an intermetallic compound. In considering the observation of an Fe_2Mo type of precipitate by X-ray and EDX analyses, it was concluded that the $(FeCr)_2Mo$ type of precipitate increases with aging time.

The change of precipitate morphology with aging

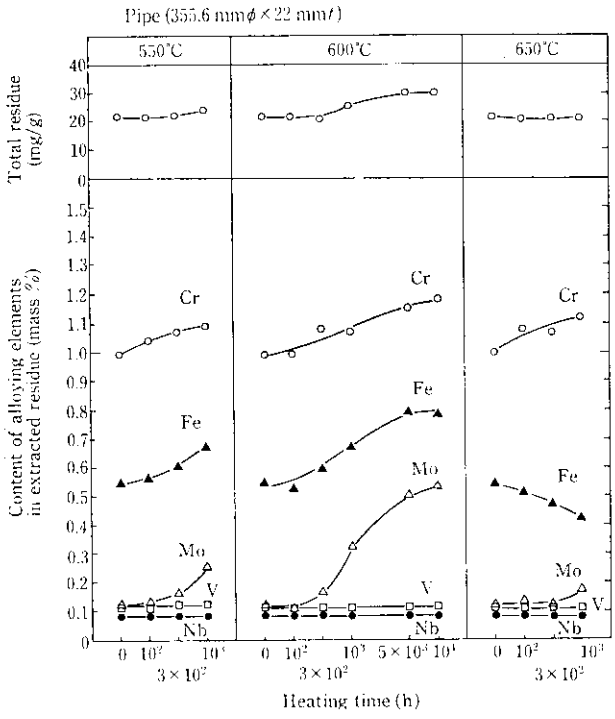

Fig. 11 Change in amount of alloying elements in extracted residue after aging

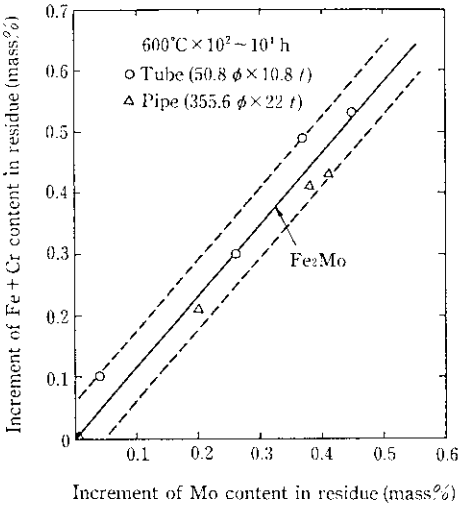

Fig. 12 Relation between increment of Mo and increment of Fe + Cr contents in residue

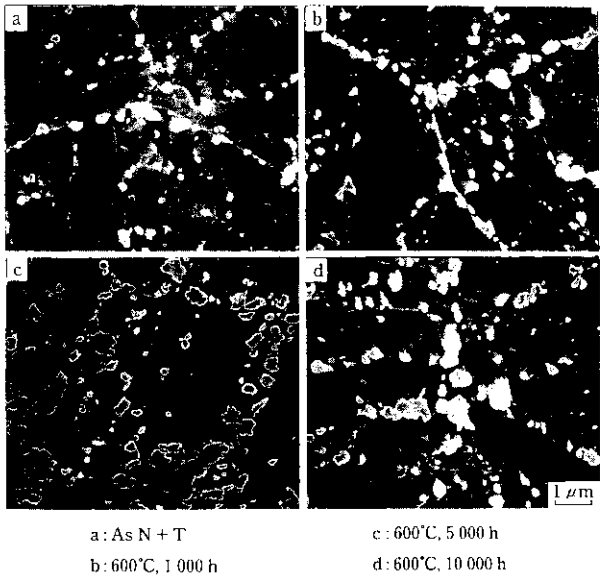

a : As N + T
b : 600°C, 1 000 h
c : 600°C, 5 000 h
d : 600°C, 10 000 h

Photo 4 Change of precipitate morphology with aging

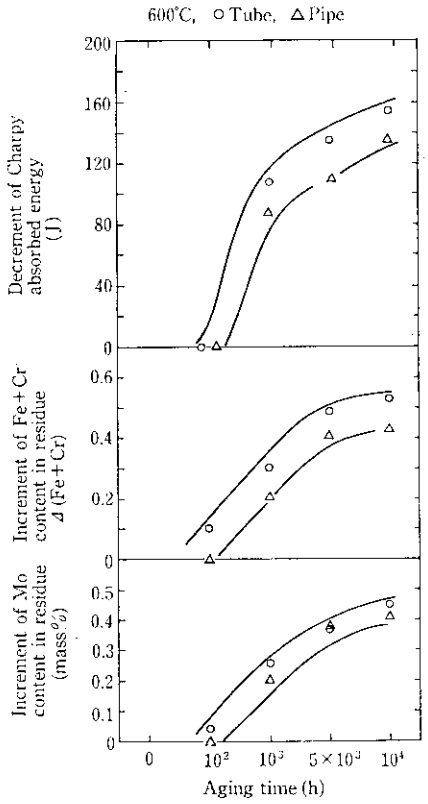

Fig. 13 Change in Charpy absorbed energy and Fe + Cr and Mo contents in residue with aging time

time at 600°C is shown in **Photo 4** from SEM observation. The number of large precipitates increased with aging time, and they were found more at the pre-austenitic grain boundaries than within the grains.

The relationship between the decrement of Charpy absorbed energy and the increment of Mo content in the residue with aging is shown in **Fig. 13**, indicating that the absobed energy decreased with increasing Mo content. This decrease of Charpy absorbed energy after long-term aging is ascribed to the formation of an Mo intermetallic compound, namely an $(FeCr)_2Mo$ precipitate.

Modified 9Cr-1Mo steel showed little change in its

tempered martensitic structure and hardness from long-term aging, while the formation and coarsening of the $(FeCr)_2Mo$ intermetallic compound reduced the absobed energy. However, the Charpy energy exceeded about 100J even after 10^4h, and this figure is high enough for actual service.

3.3.7 Properties of the hot-finished tube

Although the hot workability of T91 steel is poor, Kawasaki Steel has gained considerable experience in the production and application of hot-finished T91 tube by developing the Mannesmann process to prevent of scoring and to improve the dimensional accuracy.

(1) Dimensional Accuracy

The dimensional accuracy of tubes of 42.4 mmOD × 4.5 mmWT and 63.5 mmOD × 4.0 mmWT (the numbers show the aimed-for dimensional value) is shown in **Fig. 14**. The figures satisfy well the ASTM specifications, and the cross-sectional dimensions are particularly good as shown in **Photo 5**.

(2) Mechanical Properties

Tensile test results for the 42.4 mmOD × 4.5 mmWT tube at room temperature are shown in **Fig. 15**. These figures are at the same levels as those of the cold-finished tube with TS of 676 MPa, 0.2% PS of 529 MPa, and El of 38% on average. The impact properties of a half-size specimen are shown in **Fig. 16**. The energy value and transition temperature are equal to those of the cold-finished tube, for which the shelf energy was about 260J and the transition temperature was −55°C.

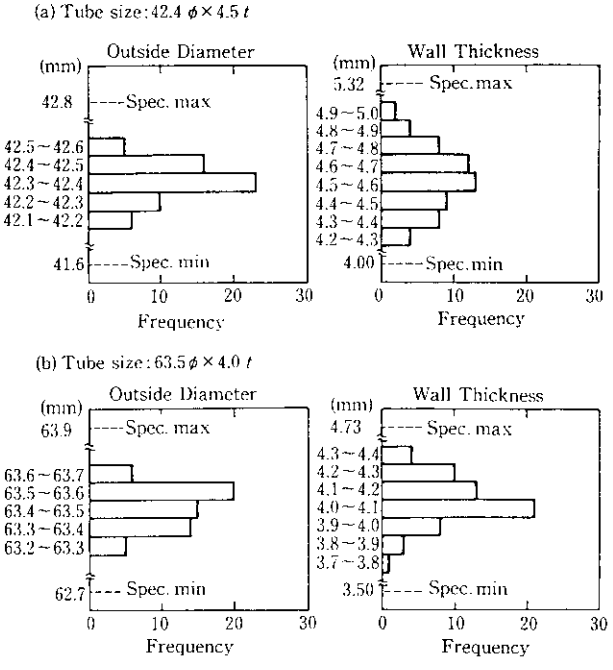

Fig. 14 Dimensional accuracy of hot-finished tubes

(mm)

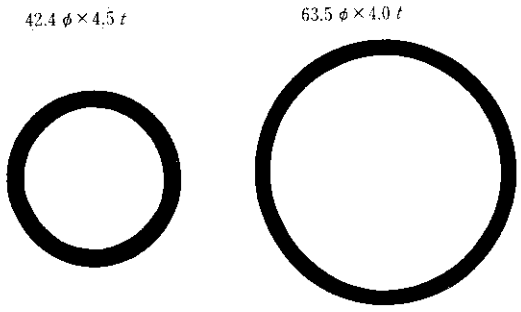

	O.D.	W.T.		O.D.	W.T.
Max.	42.42	4.67	Max.	63.51	4.23
Min.	42.30	4.43	Min.	63.39	3.98
Av.	42.37	4.56	Av.	63.46	4.11

Photo 5 Cross sectional stamps of hot-finished tubes

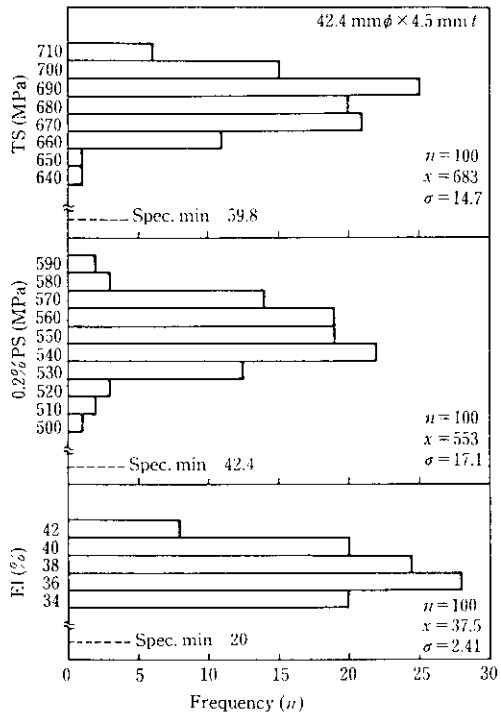

Fig. 15 Tensile properties of hot-finished tubes

Creep rupture test results for the hot-finished tube are shown in Fig. 5, indicating that both are equivalent. The appearance of the flattened and flared test specimens is shown in **Photo 6**, indicating good formability.

Modified 9Cr-1Mo steel exhibited no difference in mechanical properties between cold-finished tube and hot-finished tube, and in equivalent properties between the laboratory scale and industrial scale, due to the uniform martensitic structure achieved by normalizing. Hot-finished tube is expected to be used more due to its economic advantages.

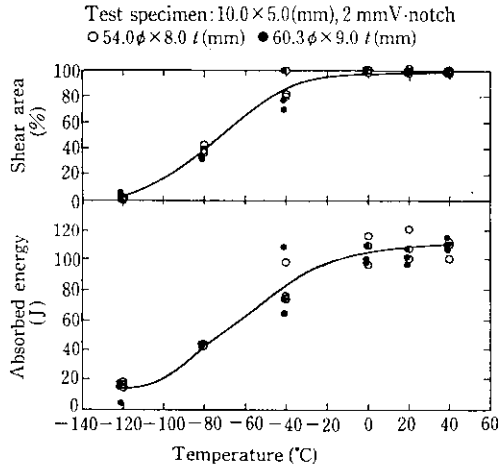

Fig. 16 Charpy absorbed energy of hot-finished tubes

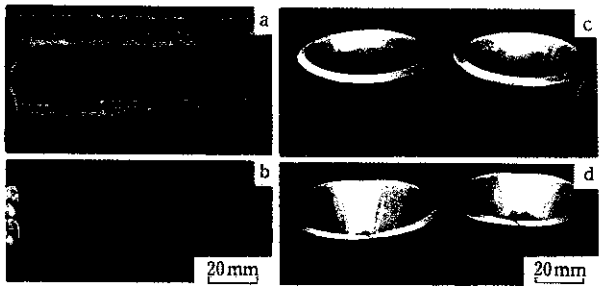

Flattening test
a : First step, no crack
b : Second step (contact), no crack

Flaring test
c : First step, no crack
Expansion rate = 1.19
d : Second step (crack initiation)
Eepansion rate = 1.95

Photo 6 Appearance of flattening- and flaring-tested specimens of hot-finished tubes

4 Conclusions

The properties of modified 9Cr-1Mo steel pipe and tube produced by the Mannesmann process were studied. The results obtained are as follows:

(1) By reducing the S content, optimizing the rolling conditions, and applying the proper heat treatment, steel tube and pipe manufactured by the Mannesmann process had excellent high-temperature properties.

(2) The mechanical and impact properties of welded joints were also outstanding.

(3) Modified 9Cr-1Mo steel showed little change in its tempered martensitic structure and hardness after long-term aging, while the formation and coarsening of an $(FeCr)_2Mo$ intermetallic compound reduced the absorbed energy. However, the Charpy energy was still about 100J even after 10^4h, which is high enough for actual service.

(4) Hot-finished tube was no different in its mechanical properties from cold-finished tube, and its dimensional accuracy was also just as good. It is expected that hot-finished tube will be used more widely in future.

References

1) T. Daikoku, F. Masuyama, H. Fujimura, H. Haneda, F. Nanjou, and T. Tuchiya: *Mitsubishi Juko Giho*, **22**(1985)4, 543
2) R. Ishimoto, I. Kajigaya, H. Umaki, and O. Abiko: *The Thermal and Nuclear Power*, **36**(1985)9, 931
3) F. Masuyama, H. Haneda, S. Kaneko, and R. Toyoda: *Mitusbishi Juko Giho*, **24**(1987)5, 491
4) T. Kanero, H. Tachibana, T. Shiraishi, S. Murase, K. Hattori, and K. Matsuo: *NKK Technical Review*, **51**(1987), 28
5) A. Iseda, M. Kubota, Y. Hayase, S. Yamamoto, and K. Yoshikawa: *The Sumitomo Search*, **36**(1988), 17
6) T. Sasaki, K. Kobayashi, T. Yamaura, O. Maeda, and K. Okita: *Tetsu-to-Hagané*, **73**(1987)13, S1341
7) T. Sasaki, K. Kobayashi, T. Yamaura, O. Maeda, and K. Okita: *CAMP-ISIJ*, **2**(1989), 1812
8) Y. Sayama: *Kawasaki Steel Giho*, **22**(1990)4, 219
9) A. Iseda, H. Teranishi, K. Yoshikawa, and T. Yukitoshi: Report of the 123rd Committee, JSPS, **25**(1984)1, 1
10) A. Iseda, H. Teranishi, and K. Yoshikawa: Report of the 123rd Committee, JSPS, **26**(1985)2, 121
11) K. Asakura, and T. Fujita: Report of the 123rd Committee, JSPS, **26**(1985)3, 467
12) A. Iseda, K. Yoshikawa, and H. Teranishi: Report of the 123rd Committee, JSPS, **27**(1986)1, 39
13) A. Iseda, H. Teranishi, K. Yoshikawa, f. Masuyama, T. Daikoku, and H. Haneda: Report of the 123rd Committee, JSPS, **29**(1988)1, 15
14) H. Hayakawa, Y. Ihara, and M. Tamura: *Tetsu-to-Hagané*, **73**(1987)13, S1341
15) T. Sasaki, K. Kobayashi, K. Okita, and O. Maeda: Report of the 123rd Committee, JSPS, **31**(1990)3, 393